JACS
JOURNAL OF THE AMERICAN CHEMICAL SOCIETY

Subscriber access provided by American Chemical Society

Article

Oxidation of C–H Bonds by [(bpy)(py)RuO]$^{2+}$ Occurs by Hydrogen Atom Abstraction

Jasmine R. Bryant, and James M. Mayer

J. Am. Chem. Soc., **2003**, 125 (34), 10351-10361• DOI: 10.1021/ja035276w • Publication Date (Web): 02 August 2003

Downloaded from http://pubs.acs.org on March 29, 2009

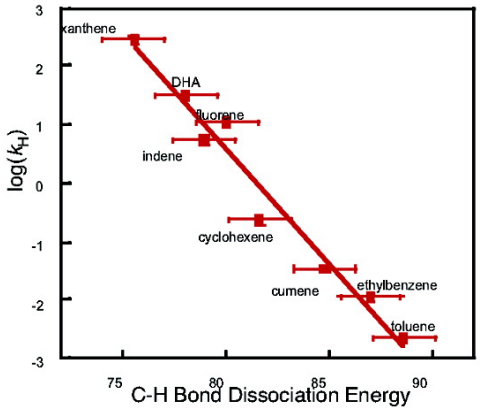

correlation of $k_{H\text{-atom transfer}}$ with C–H bond strength

More About This Article

Additional resources and features associated with this article are available within the HTML version:

- Supporting Information
- Links to the 9 articles that cite this article, as of the time of this article download
- Access to high resolution figures
- Links to articles and content related to this article
- Copyright permission to reproduce figures and/or text from this article

View the Full Text HTML

ACS Publications
High quality. High impact.

Journal of the American Chemical Society is published by the American Chemical Society. 1155 Sixteenth Street N.W., Washington, DC 20036

J|A|C|S
ARTICLES
Published on Web 08/02/2003

Oxidation of C−H Bonds by $[(bpy)_2(py)Ru^{IV}O]^{2+}$ Occurs by Hydrogen Atom Abstraction

Jasmine R. Bryant and James M. Mayer*

Contribution from the Department of Chemistry, Campus Box 351700, University of Washington, Seattle, Washington 98195-1700

Received March 21, 2003; E-mail: mayer@chem.washington.edu.

Abstract: Anaerobic oxidations of 9,10-dihydroanthracene (DHA), xanthene, and fluorene by $[(bpy)_2(py)Ru^{IV}O]^{2+}$ in acetonitrile solution give mixtures of products including oxygenated and non-oxygenated compounds. The products include those formed by organic radical dimerization, such as 9,9′-bixanthene, as well as by oxygen-atom transfer (e.g., xanthone). The kinetics of these reactions have been measured. The kinetic isotope effect for oxidation of DHA vs DHA-d_4 gives $k_H/k_D \geq 35 \pm 1$. The data indicate a mechanism of initial hydrogen-atom abstraction forming radicals that dimerize, disproportionate and are trapped by the oxidant. This mechanism also appears to apply to the oxidations of toluene, ethylbenzene, cumene, indene, and cyclohexene. The rate constants for H-atom abstraction from these substrates correlate well with the strength of the C−H bond that is cleaved. Rate constants for abstraction from DHA and toluene also correlate with those for oxygen radicals and other oxidants. The rate constant for H-atom transfer from toluene to $[(bpy)_2(py)Ru^{IV}O]^{2+}$ appears to be close to that predicted by the Marcus cross relation, using a tentative rate constant for hydrogen atom self-exchange between $[(bpy)_2(py)Ru^{III}OH]^{2+}$ and $[(bpy)_2(py)Ru^{IV}O]^{2+}$.

Introduction

Selective oxidations of organic compounds, including oxidations of C−H bonds, are of fundamental, technological, and biochemical interest.[1] Ruthenium-oxo compounds have received particular attention in this area.[2−22] Over the past twenty-five years, Meyer and co-workers,[3−20] and others,[21,22] have shown that ruthenium-oxo-polypyridyl complexes such as $[(bpy)_2(py)Ru^{IV}O]^{2+}$ (**RuO**$^{2+}$) are powerful and versatile oxidants. The properties of **RuO**$^{2+}$ and its related hydroxo and aquo derivatives, $[(bpy)_2(py)Ru^{III}OH]^{2+}$ (**RuOH**$^{2+}$) and $[(bpy)_2(py)Ru^{II}OH_2]^{2+}$ (**RuOH$_2$**$^{2+}$), have been described in detail.[20] **RuO**$^{2+}$ has been reported to oxidize substrates by a variety of mechanisms, including electron transfer,[4] proton-coupled electron transfer,[5−7] hydrogen atom abstraction,[8,9] hydride abstraction,[10−13] and oxygen atom transfer (including epoxidation).[14−18] The

(1) (a) Olah, G. A.; Molnár, Á. *Hydrocarbon Chemistry*; Wiley: New York, 1995; pp 375ff. (b) Shilov, A. E.; Shul′pin, G. B. *Activation and Catalytic Reactions of Saturated Hydrocarbons in the Presence of Metal Complexes*; Kluwer: Boston, 2000. (c) *Biomimetic Oxidations Catalyzed by Transition Metal Complexes*; Meunier, B., Ed.; Imperial College Press: London, 2000.
(2) Reviews: (a) Giffith, W. P. *Chem. Soc. Rev.* **1992**, 179−185. (b) Che, C.-M.; Yam, V. W. W. *Adv. Trans. Met. Chem.* **1996**, *1*, 209−237. (c) Courtney, J. L. In *Organic Syntheses By Oxidation With Metal Compounds*; Mijs, W. J., de Jonge, C. R. H. I., Eds.; Plenum Press: New York, 1986; 445−467.
(3) (a) Meyer, T. J. *J. Electrochem. Soc.* **1984**, *131*, 221C. (b) Moyer, B. A.; Meyer, T. J. *J. Am. Chem. Soc.* **1978**, *100*, 3601−3603.
(4) Lebeau, E. L.; Binstead, R. A.; Meyer, T. J. *J. Am. Chem. Soc.* **2001**, *123*, 10 535−10 544.
(5) Binstead, R. A.; McGuire, M. E.; Dovletoglou, A.; Seok, W. K.; Roecker, L. E.; Meyer, T. J.*J. Am. Chem. Soc.* **1992**, *114*, 173−186.
(6) Binstead, R. A.; Stultz, L. K.; Meyer, T. J. *Inorg. Chem.* **1995**, *34*, 546−551.
(7) Trammell, S. A.; Wimbish, J. C.; Odobel, F.; Gallagher, L. A.; Narula, P. M.; Meyer, T. J. *J. Am. Chem. Soc.* **2001**, *120*, 13 248−13 249.
(8) Binstead, R. A.; Meyer, T. J. *J. Am. Chem. Soc.* **1987**, *109*, 3287−3297.
(9) (a) Gilbert, J.; Roecker, L.; Meyer, T. J. *Inorg. Chem.* **1987**, *26*, 1126−1132. (b) Gilbert, J. A.; Gersten, S. W.; Meyer, T. J. *J. Am. Chem. Soc.* **1982**, *104*, 6872−6873.
(10) Thompson, M. S.; Meyer, T. J. *J. Am. Chem. Soc.* **1982**, *104*, 5070−5076.
(11) Roecker, L. E.; Meyer, T. J. *J. Am. Chem. Soc.* **1986**, *108*, 4066−4073.
(12) Roecker, L. E.; Meyer, T. J. *J. Am. Chem. Soc.* **1987**, *109*, 746−754.
(13) Thompson, M. S.; Meyer, T. J. *J. Am. Chem. Soc.* **1982**, *104*, 4106−4115.
(14) Seok, W. K.; Meyer, T. J. *J. Am. Chem. Soc.* **1988**, *110*, 7358−7367.
(15) (a) Roecker, L.; Dobson, J. C.; Vining, W. J.; Meyer, T. J. *Inorg. Chem.* **1987**, *26*, 779−781. (b) Moyer, B. A.; Sipe, K.; Meyer, T. J. *Inorg. Chem.* **1981**, *20*, 1475−1480.
(16) Seok, W. K.; Dobson, J. C.; Meyer, T. J. *Inorg. Chem.* **1988**, *27*, 3−5.
(17) (a) Stultz, L. K.; Binstead, R. A.; Reynolds, M. S.; Meyer, T. J. *J. Am. Chem. Soc.* **1995**, *117*, 2520−2532. (b) The rate constant for oxidation of indene to indenone is reported here as 5.74 ± 0.4 M^{-1} s^{-1}, including a stoichiometric factor of 2 to account for the consumption of 2 **RuO**$^{2+}$ per indanone.
(18) Stultz, L. K.; Huynh, M. H. V.; Binstead, R. A.; Curry, M.; Meyer, T. J. *J. Am. Chem. Soc.* **2000**, *122*, 5984−5996.
(19) (a) Curry, M.; Huynh, M. H. V.; Stultz, L. K.; Binstead, R. A.; Meyer, T. J., personal communication. (b) Bryant, J. R.; Mayer, J. M., manuscript in preparation.
(20) (a) Moyer, B. A.; Meyer, T. J. *Inorg. Chem.* **1981**, *20*, 436−444. (b) Dobson, J. C.; Helms, J. H.; Doppelt, P.; Sullivan, B. P.; Hatfield, W. E.; Meyer, T. J. *Inorg. Chem.* **1989**, *28*, 2200−2204. (c) The potentials vs SCE in ref 20a have been converted to NHE by adding 0.24 V.
(21) Representative papers and leading references: (a) Yamada, H.; Hurst, J. K. *J. Am. Chem. Soc.* **2000**, *122*, 5303−5311. (b) Farrer, B. T.; Thorp, H. H. *Inorg. Chem.* **1999**, *38*, 2497−2502. (c) Muller, J. G.; Acquaye, J. H.; Takeuchi, K. J. *Inorg. Chem.* **1992**, *31*, 4552−4557. (d) Gerli, A.; Reedijk, J.; Lakin, M. T.; Spek, A. L.; *Inorg. Chem.* **1995**, *34*, 1836−1843. (e) Goldstein, A. S.; Beer, R. H.; Drago, R. S. *J. Am. Chem. Soc.* **1994**, *116*, 2424−2429. (f) Dengel, A. C.; El-Hendawy, A. M.; Griffith, W. P.; O'Mahoney, C. A.; Williams, D. J. *J. Chem. Soc., Dalton Trans.* **1990**, 737. (g) Kojima, T. *Chem. Lett.* **1996**, 121−122. (g) Hua, X.; Lappin, A. G. *Inorg. Chem.* **1995**, *34*, 992−994. (h) Lau, T. C.; Kochi, J. K. *J. Chem. Soc., Chem. Commun.* **1987**, 798−799. (i) Huynh, M. H. V.; Witham, L. M.; Lasker, J. M.; Wetzler, M.; Mort, B.; Jameson, D. L.; White, P. S.; Takeuchi, K. J.; *J. Am. Chem. Soc.* **2003**, 308−309.
(22) cf., (a) Che, C.-M.; Yu, W.-Y.; Chan, P.-M.; Cheng, W.-C.; Peng, S.-M.; Lau, K.-C.; Li, W.-K.; *J. Am. Chem. Soc.* **2000**, *122*, 11 380−11 392. (b) Che, C.-M.; Cheng, K.-W.; Chan, M. C. W.; Lau, T.-C.; Mak, C.-K. *J. Org. Chem.* **2000**, *65*, 7996−8000. (c) Che, C.-M.; Ho, C.; Lau, T. C. *J. Chem. Soc., Dalton Trans.* **1991**, 1901. (d) Che, C.-M.; Tang, W. T.; Wong, K.-Y.; Li, C.-K. *J. Chem. Soc., Dalton Trans.* **1991**, 3277.

Scheme 1. Thermochemical Data in the $[(bpy)_2(py)Ru^{IV}O]^{2+}$ System ($E°$ vs NHE, pK_a Values[4,20])

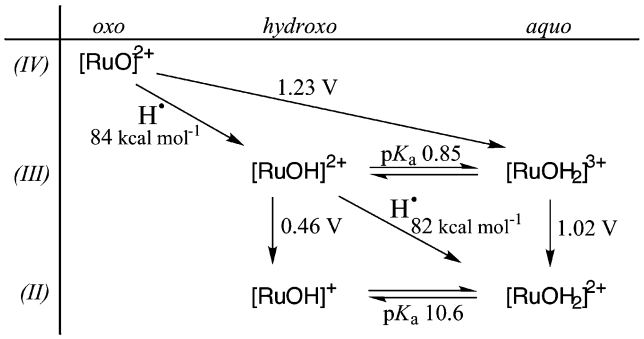

reactions studied have involved the oxidation of O−H bonds (H_2O_2,[9] alcohols,[12,13] and hydroquinone[5]) as well as oxidations of C−H bonds. The oxidations of allylic C−H bonds in indene and cyclohexene have been proposed to occur by direct oxygen-atom insertion.[16,18] Oxidations of cumene, ethylbenzene, and toluene were suggested to occur by a nucleophile-assisted hydride transfer mechanism,[10] although this conclusion is not supported by recent results in our lab and in the Meyer lab.[19] In this report, we present evidence that all of the C−H bond oxidations occur by a mechanism of initial hydrogen atom transfer from the benzylic or allylic C−H bond to the oxo group of $\mathbf{RuO^{2+}}$.

Work in our lab and elsewhere has shown that, in general, the ability of a metal complex to abstract a hydrogen atom from a substrate correlates with the thermodynamic driving force for H-atom transfer.[23−25] This correlation is a subset of the more general result that H-atom transfer reactions typically follow the Marcus cross relation, identifying the importance of both driving force and intrinsic barriers.[26] For a reaction X + HY → HX + Y, the $\Delta H°$ is the difference between the bond dissociation energies of HX and HY. The H−X bond strength can be determined from the redox potential of X and the pK_a of HX (or the $E°$ for HX and the pK_a of HX^+), using thermochemical cycles.[27−30] The enthalpies for $\mathbf{RuO^{2+}} + H \rightarrow \mathbf{RuOH^{2+}}$ and $\mathbf{RuOH^{2+}} + H \rightarrow \mathbf{RuOH_2^{2+}}$ in aqueous solution can be calculated via this approach (Scheme 1) using the potential and pK_a data reported by Meyer et al.[20] In this somewhat unusual case, the Ru^{IV}/Ru^{III} reduction potential at pH 0 corresponds to a one electron-two proton process forming $\mathbf{RuOH_2^{3+}}$, whose pK_a must be subtracted to get the thermodynamics for one electron-one proton (hydrogen atom) transfer.[31]

(23) (a) Mayer, J. M. *Acc. Chem. Res.* **1998**, *31*, 441−450. (b) Roth, J. P.; Mayer, J. M. *Inorg. Chem.* **1999**, *38*, 2760−2761. (c) Larsen, A. S.; Wang, K.; Lockwood, M. A.; Rice, G. L.; Won, T.-J.; Lovell, S.; Sadílek, M.; Tureek, F.; Mayer, J. M. *J. Am. Chem. Soc.* **2002**, *124*, 10 112−10 123.
(24) See, for example, (a) Bakac, A. *J. Am. Chem. Soc.* **2000**, *122*, 1092−1097. (b) Strassner, T.; Houk, K. N. *J. Am. Chem. Soc.* **2000**, *122*, 7821−7822.
(25) For an exception to the correlation of H-atom transfer rate with bond strength, see: Goldsmith, C. R.; Jonas, R. T.; Stack, T. D. P. *J. Am. Chem. Soc.* **2002**, *124*, 83−96.
(26) (a) Roth, J. P.; Yoder, J. C.; Won, T.-J.; Mayer, J. M. *Science* **2001**, *294*, 2524−2526. (b) Roth, J. P.; Lovell, S.; Mayer, J. M. *J. Am. Chem. Soc.* **2000**, *122*, 5486−5498.
(27) (a) Bordwell, F. G.; Cheng, J.-P.; Ji, G.-Z.; Satish, A. V.; Zhang, X. *J. Am. Chem. Soc.* **1991**, *113*, 9790−9795. (b) Bordwell, F. G.; Cheng, J.-P.; Harrelson, J. A., Jr. *J. Am. Chem. Soc.* **1988**, *110*, 1229−1231. (c) Zhang, X.-M.; Bordwell, F. G. *J. Am. Chem. Soc.* **1992**, *114*, 7458−7462.
(28) (a) Parker, V. D.; Handoo, K. L.; Roness, F.; Tilset, M. *J. Am. Chem. Soc.* **1991**, *113*, 7493−7498. (b) Parker, V. D. *J. Am. Chem. Soc.* **1992**, *114*, 7458−7462; and correction: Parker, V. D. *J. Am. Chem. Soc.* **1993**, *115*, 1201.
(29) Gardner, K. A.; Kuehnert, L. L.; Mayer, J. M. *Inorg. Chem.* **1997**, *36*, 2069−2078.
(30) Mayer, J. M. In ref 1c, pp 1−43.

Table 1. Yields of Products Formed from the Oxidation of DHA by $\mathbf{RuO^{2+}}$[a]

$[RuO^{2+}]$:[DHA]	[anthrone]	[anthraquinone]	[anthracene]	total (%)
1:1	0.06 (12%)	0.06 (24%)	0.39 (39%)	75
1:2	0.11 (22%)	0.05 (20%)	0.55 (55%)	97
1:4	0.09 (18%)	0.03 (12%)	0.70 (70%)	100
1:10	0.09 (18%)	*b*	0.87 (87%)	105
2:4	0.17 (17%)	0.11 (22%)	1.10 (55%)	94
4:4	0.30 (15%)	0.30 (30%)	1.33 (33%)	78

[a] Reagent amounts and yields in mM (accurate to ± ∼10%); DHA = 9,10-dihydroanthracene. Values in parentheses are the percentages of the total $\mathbf{RuO^{2+}}$ oxidative equivalents consumed in the formation of this product. [b] <0.01 (<4%).

Reported here are studies of the oxidations of 9,10-dihydroanthracene (DHA), xanthene, fluorene, and related substrates by $\mathbf{RuO^{2+}}$. Both product and kinetic studies support a common mechanism of hydrogen atom transfer followed by competitive radical dimerization and radical trapping by the oxidant. There is a clear correlation between the rate constant for H-atom abstraction and the C−H bond dissociation energy (BDE) of the organic substrate, both for the compounds studied here and for the oxidations of other benzylic and allylic substrates. In addition, the hydrogen-atom self-exchange rate for $\mathbf{RuO^{2+}} + \mathbf{RuOH^{2+}}$ has been probed by dynamic ^1H NMR line-broadening, to apply the Marcus cross relation to these reactions.

Results

Oxidations of Organic Substrates and Product Characterization. The oxidations of DHA, xanthene, and fluorene by $\mathbf{RuO^{2+}}$ were carried out anaerobically at room temperature in dry acetonitrile, typically with 1−2 mM $\mathbf{RuO^{2+}}$ and 1−10 mM substrate. Reactions are complete within minutes and a mixture of organic products is observed for each reaction. Organic products were characterized by GC/MS and quantitated using calibrated GC/FID response factors with naphthalene as an internal standard. Yields are reproducible in samples analyzed after extended periods of time (6−24 h). The inorganic products were characterized by UV−vis and/or NMR spectroscopies.

DHA is oxidized within seconds to give a mixture of anthracene, anthrone, and anthraquinone, with anthracene as the major product (eq 1, Table 1). The product distributions are dependent on initial concentrations of oxidant and substrate (see below). To determine the source of oxygen in the oxygenated products, reactions were carried out with 10 mM added $H_2{}^{18}O$. It has been shown that $\mathbf{RuO^{2+}}$ does not exchange with $H_2{}^{18}O$ in water over the time scale of these reactions.[15b] Anthraquinone shows 2% ^{18}O incorporation by GC/MS from the intensity of the $(M + 2)^+$ vs M^+ ions in comparison to reactions in which no labeled water was added. No incorporation into anthrone was detected.

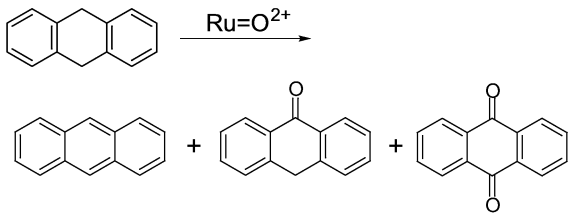

(1)

Xanthene reacts with $\mathbf{RuO^{2+}}$ within seconds to give a mixture of xanthone, the major product, and 9,9′-bixanthene (eq 2, Table 2). Oxidation of fluorene proceeds similarly, about an order of

Table 2. Yields of Products Formed from the Oxidations of Xanthene and Fluorene (YH_2) by $\mathbf{RuO^{2+}}$[a]

$[RuO^{2+}]:[YH_2]$	[Y=O]	$[(YH)_2]$	total (%)
xanthene: 1:1	0.36 (72%)	0.013 (1.3%)	73
1:2	0.35 (70%)	0.019 (1.9%)	72
1:4	0.31 (62%)	0.025 (2.5%)	65
1:10	0.38 (76%)	0.036 (3.6%)	80
2:4	0.66 (66%)	0.045 (2.3%)	68
4:4	1.31 (66%)	0.045 (1.1%)	67
fluorene: 1:1	0.37 (74%)	0.011 (1.1%)	75
1:2	0.33 (66%)	0.014 (1.4%)	67
1:4	0.31 (62%)	0.017 (1.7%)	64
1:10	0.33 (66%)	0.023 (2.3%)	68
2:4	0.63 (66%)	0.027 (1.4%)	67
4:4	1.25 (63%)	0.027 (0.7%)	64

[a] Reagent amounts and yields in mM (±10%). Values in parentheses are the percentages of the total $\mathbf{RuO^{2+}}$ oxidative equivalents consumed in the formation of this product. Y=O is xanthone or fluorenone; $(YH)_2$ = bixanthene or bifluorene.

magnitude slower than xanthene. This reaction produces fluorenone, bifluorene and a very small amount of bifluorenylidene, with fluorenone as the major product (eq 3, Table 2). Oxidations in the presence of 10 mM $H_2{}^{18}O$ give essentially unlabeled ketones: 2% ^{18}O in the xanthone and <1% ^{18}O in the fluorenone.

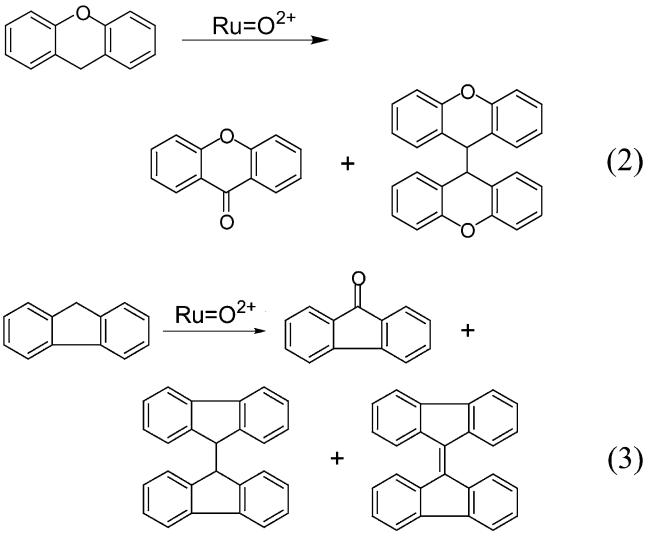

The ruthenium products of these reactions appear to be a mixture of mostly $\mathbf{RuOH_2^{2+}}$ and the known acetonitrile complex $[(bpy)_2(py)Ru^{II}(NCMe)]^{2+}$ ($\mathbf{RuNCMe^{2+}}$).[6] The mixture quantitatively converts over time to $\mathbf{RuNCMe^{2+}}$ as the aquo complex undergoes solvolysis ($k_{solv} = 1.66 \times 10^{-3}$ s^{-1}; $t_{1/2} = 7$ min).[6] After several hours, 100% conversion of $\mathbf{RuO^{2+}}$ to $\mathbf{RuNCMe^{2+}}$ is observed by UV−vis spectroscopy (λ_{max} 440 nm, $\epsilon = 8160$ M^{-1} cm^{-1}).[6]

Anthrone is oxidized by $\mathbf{RuO^{2+}}$ within seconds to form anthraquinone (quantitatively by GC/FID) and a mixture of $\mathbf{RuOH_2^{2+}}$ and $\mathbf{RuNCMe^{2+}}$ (by UV−vis). The analogous oxidation of anthracene is much slower, requiring 30 min at room temperature (vs 5 s for DHA). At 2 mM $\mathbf{RuO^{2+}}$ and 4 mM anthracene, 0.47 mM anthraquinone is produced. Conversion of anthracene to anthraquinone is a six-electron oxidation, requiring 3 equiv of $\mathbf{RuO^{2+}}$ per quinone formed. Thus, the observed yield accounts for 71% of the $\mathbf{RuO^{2+}}$ oxidative equivalents consumed. The ruthenium product of this reaction appears to be only $\mathbf{RuNCMe^{2+}}$. No $\mathbf{RuOH_2^{2+}}$ is observed by UV−vis, consistent with the time scale of the reaction being longer than that for solvolysis.

In the oxidations of DHA, xanthene and fluorene, the ratios of organic products depend on the initial $\mathbf{RuO^{2+}}$ and substrate concentrations, as shown in Tables 1 and 2. In each table, the percentage yields are given in terms of oxidative equivalents. This value is the concentration of the organic product times the number of $\mathbf{RuO^{2+}}$ equivalents required to produce it, dividing by the initial concentration of $\mathbf{RuO^{2+}}$. In the oxidation of DHA, for instance, 1 equiv of $\mathbf{RuO^{2+}}$ is consumed for each anthracene, 2 for anthrone, and 4 for anthraquinone. The final columns give the percentage of $\mathbf{RuO^{2+}}$ oxidative equivalents accounted for by the products listed. Less than quantitative total yields here and elsewhere may be due in part to the slow decomposition of $\mathbf{RuO^{2+}}$ during storage and in solution, or to the formation of products such as carboxylic acids which would not have been observed with the GC conditions used. In the DHA oxidations, the percentage yield of anthraquinone decreases with increasing [DHA] at constant [$\mathbf{RuO^{2+}}$] (the first four entries in Table 1). Conversely, comparing the three entries with 4 mM DHA, the yield of anthraquinone increases with increasing [$\mathbf{RuO^{2+}}$].

In the reactions of $\mathbf{RuO^{2+}}$ with xanthene and fluorene, the products account for 64−80% of the ruthenium oxidative equivalents consumed (Table 2). The remaining $\mathbf{RuO^{2+}}$ may be consumed by further oxidation of bixanthene or bifluorene, whose tertiary benzylic C−H bonds should be quite reactive. A trace of bifluorenylidene is observed in the fluorene oxidations. The coupled products, bixanthene and bifluorene, are formed in low yields of 1−3% (estimated errors ±∼30% of these values). The yields of these products are larger with lower ruthenium and higher substrate concentrations, as will be discussed below using a kinetic model.

Kinetics. The kinetics of the reactions of $\mathbf{RuO^{2+}}$ with DHA, anthracene, xanthene, fluorene, indene, cyclohexene, and toluene were measured by UV−vis spectroscopy at 24 °C in acetonitrile under a nitrogen atmosphere. Reactions with cumene and ethylbenzene will be described elsewhere.[19] The organic substrate was always in large excess (pseudo-first-order conditions). Reactions with DHA, xanthene, fluorene, indene, and cyclohexene were fast enough to require measurements with a stopped-flow instrument. Anthracene kinetics were measured on a diode array UV−vis spectrophotometer over 30 min; reactions with toluene required several hours to reach completion, even with 2500-fold excess substrate (0.5 M). $\mathbf{RuO^{2+}}$ is known to decompose slowly in acetonitrile (over 24 h or more),[6] but not appreciably during the time scale of kinetic measurements.

Kinetics traces were fitted with SPECFIT,[32] a global analysis software package. The rapid reactions with DHA, xanthene and indene could be fit with a biexponential model A → B → C. The slower reaction of $\mathbf{RuO^{2+}}$ with fluorene requires a triexponential model, A → B → C → D. SPECFIT calculates spectra for A, B, C, and D, which can then be interpreted using the known spectral properties in this system (see Figures 1−3, Supporting Information Figure S1). The spectra calculated for

(31) In this case, BDE = 23.06 $E°$ − 1.37 pK_a − C where $E°$ (vs NHE) and pK_a are measured in water and $C = -57 \pm 2$.[29,30]

(32) Spectrum Software Associates, Marlborough, MA.

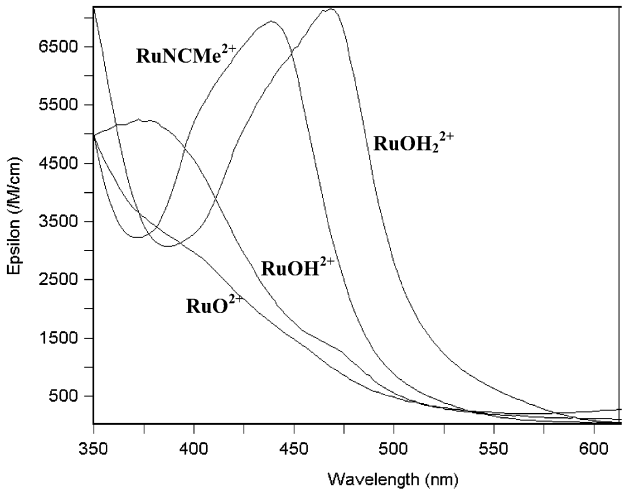

Figure 1. Spectra of $\mathbf{RuO^{2+}}$, $\mathbf{RuOH^{2+}}$ (spectra obtained from a 1:1 mixture of $\mathbf{RuO^{2+}}$, and $\mathbf{RuOH_2^{2+}}$, contains a slight amount of $\mathbf{RuOH_2^{2+}}$), $\mathbf{RuOH_2^{2+}}$, $\mathbf{RuNCMe^{2+}}$.

B, C, and D all appear to be due to mixtures of ruthenium species, and some include absorbances due to organic products. For the reactions that occur more slowly than the rate of solvolysis of $\mathbf{RuOH_2^{2+}}$, the observed final product appears to be predominantly $\mathbf{RuNCMe^{2+}}$. When the kinetics are complete in less than a few minutes, solvolysis is not a significant reaction and the final product C (or D for fluorene) appears to be a mixture of Ru^{II} species, $[(bpy)_2(py)Ru^{II}(L)]^{2+}$ where L = H_2O, MeCN, or an organic product such as xanthone. Ru^{II}-bpy complexes have a characteristic MLCT absorbance with $\epsilon \approx 8000\ M^{-1}\ cm^{-1}$, as in $\mathbf{RuOH_2^{2+}}$ (λ_{max} = 468 nm) and $\mathbf{RuNCMe^{2+}}$ (λ_{max} = 440 nm).[6] The A → B → C → D model is needed for the reaction of fluorene at least in part because the C → D step includes the solvolysis of any $\mathbf{RuOH_2^{2+}}$ that is present in C. The k_{obs} for the C → D rate depends on reagent concentrations, varying from $5.8 \times 10^{-5}\ s^{-1}$ to $7.8 \times 10^{-3}\ s^{-1}$, and is similar in magnitude to the rate constant for solvolysis, $1.66 \times 10^{-3}\ s^{-1}$.[6]

The calculated spectra for B are consistent with mixtures of Ru^{III} and Ru^{II} species. At the stage of the reaction when B is at a maximum, the xanthene reaction mixture contains a substantial amount of Ru^{II} (Figure 3). Ru^{II} species make a much smaller contribution to B in the DHA reaction (Figure 2). The Ru^{III} components of B likely include both $\mathbf{RuOH^{2+}}$ and some $[(bpy)_2(py)Ru^{III}OR]^{2+}$ species, where R is derived from the substrate (e.g., fluorenyl). Similar conclusions have been made by Meyer et al. in related systems.[17−19a]

The kinetic models yield first-order rate constants k_{obs} for each of the reaction phases. Plots of k_{obs}(A → B) vs [substrate] are linear for DHA, xanthene, and fluorene (Figure 4), giving second-order rate constants, $k = 125 \pm 8\ M^{-1}\ s^{-1}$ (DHA), $577 \pm 13\ M^{-1}\ s^{-1}$ (xanthene) and $21.9 \pm 1.8\ M^{-1}\ s^{-1}$ (fluorene). In each case, k_{obs} for the second phase (B → C) is not linearly related to substrate concentration, with values varying from 0.027 to 0.79 s^{-1} for DHA, 0.19−1.66 s^{-1} for xanthene, and 0.014−0.065 s^{-1} for fluorene. The linearity of the data in Figure 4 and the negligible intercepts indicate that the A → B phase follows the simple bimolecular rate law in eq 4. Furthermore,

$$\text{Rate} = k_{A\rightarrow B}[\mathbf{RuO^{2+}}][\text{substrate}] \qquad (4)$$

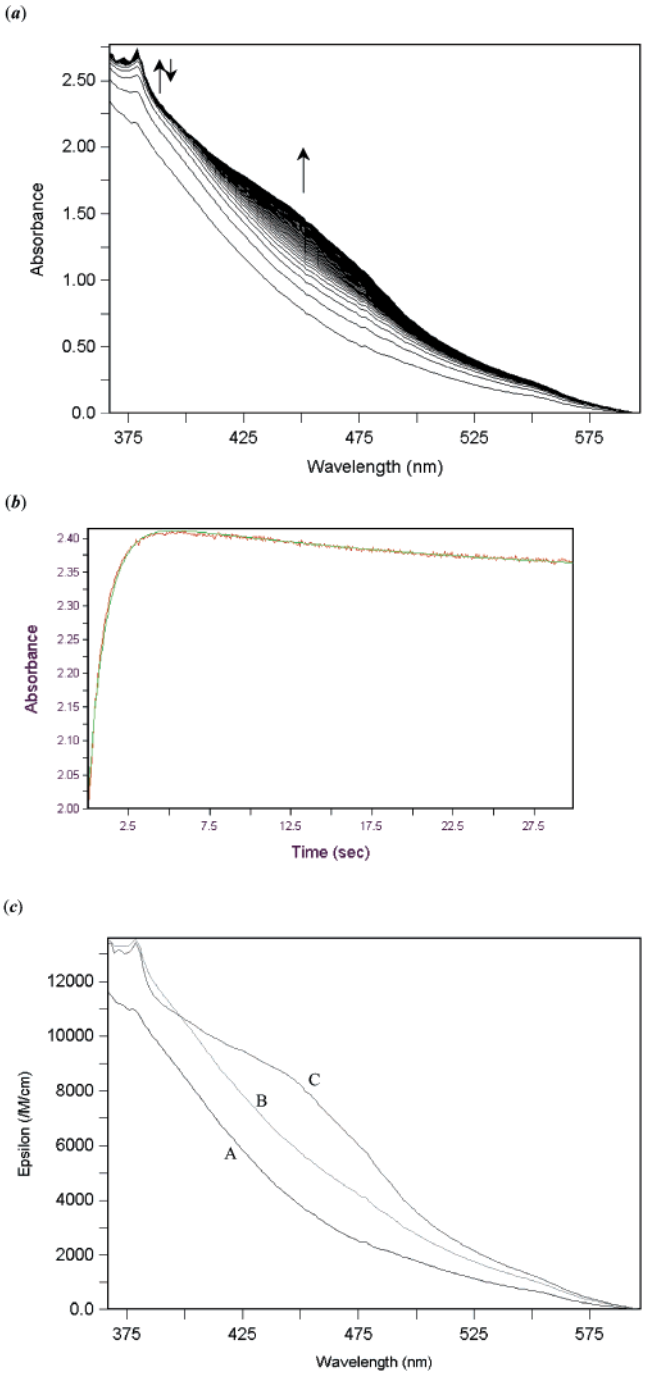

Figure 2. (a) Spectral changes observed for the reaction of 0.2 mM $\mathbf{RuO^{2+}}$ with 6 mM DHA over 30 s. (b) Single wavelength trace of the absorbance at 385.5 nm with SPECFIT fit (green) showing the initial rising A → B phase followed by the decreasing B → C phase. (c) Calculated spectra returned by SPECFIT for A, B, and C.

for all three substrates, plots of $\log k_{obs}$ vs log[substrate] are linear with slopes of 0.90−0.97 and intercepts equal to log k (Figure S2). Thus, the rate-limiting step of the A → B phase involves the bimolecular reaction of $\mathbf{RuO^{2+}}$ and substrate; subsequent reactions that form the mixture of species that make up B are fast on this time scale. Rates of oxidation of xanthene by $\mathbf{RuO^{2+}}$ were investigated from 278 to 318 K, yielding the activation parameters $\Delta H^{\ddagger} = 4.9 \pm 1.0$ kcal mol^{-1} and $\Delta S^{\ddagger} = -30 \pm 5$ cal $mol^{-1}\ K^{-1}$ (the Eyring plot is deposited as Figure S3). These values are similar in magnitude to those reported for other C−H

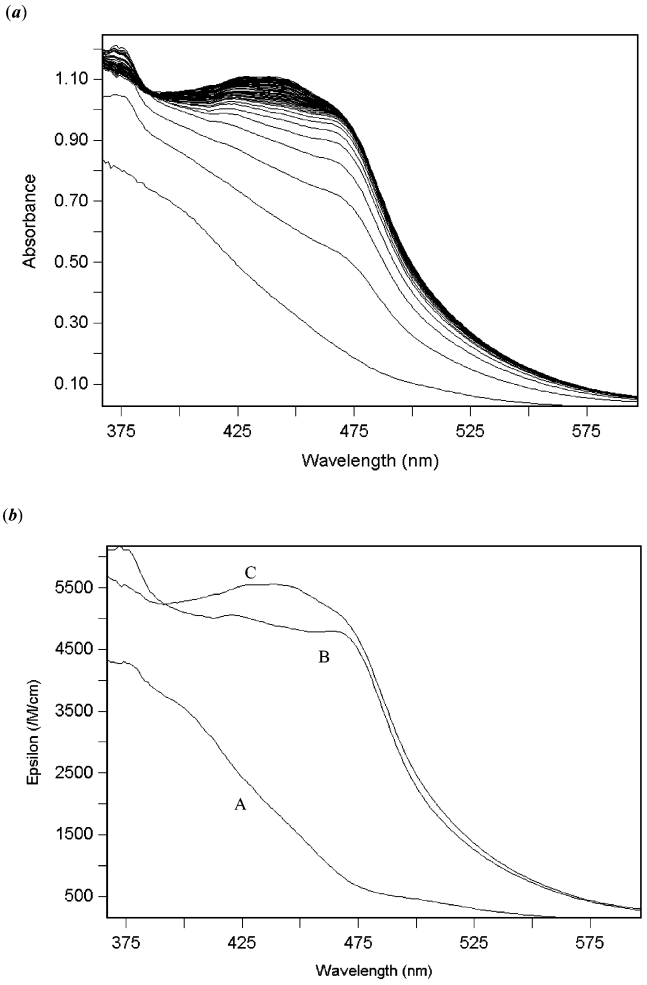

Figure 3. (a) Spectral changes observed for the reaction of 0.2 mM **RuO**$^{2+}$ with 20 mM xanthene over 3 s (1000 scans/s). (b) Calculated spectra returned by SPECFIT for A, B, and C.

bond oxidations by **RuO**$^{2+}$. For example, the oxidation of cyclohexene to 2-cyclohexen-1-one has activation parameters of $\Delta H^{\ddagger} = 7.4 \pm 0.1$ kcal mol^{-1} and $\Delta S^{\ddagger} = -34 \pm 3.4$ cal mol^{-1} K^{-1}.[18]

The kinetics of anthracene and anthrone oxidation by **RuO**$^{2+}$ were measured to determine their roles as possible intermediates in the oxidation of DHA. Spectral changes for the anthracene reactions can be fit to a single exponential (A → B model), with **RuNCMe**$^{2+}$ as the only product (Figure S4). Monitoring at 440 nm (λ_{max} for **RuNCMe**$^{2+}$) gives $k_{anth} = 0.273 \pm 0.01$ M^{-1} s^{-1}. The oxidation of anthrone by **RuO**$^{2+}$ is quite rapid—complete within the mixing delay of the stopped flow instrument. Assuming a first-order dependence on anthrone concentration and that three half-lives of the reaction are complete in 3 ms, $k_{anthrone}$ is calculated to be greater than $\sim 10^5$ M^{-1} s^{-1}. On the basis of these rate constants, the oxidation of DHA to anthrone and anthraquinone cannot proceed via oxidation of anthracene. A SPECFIT simulation of a DHA oxidation in which anthrone and anthraquinone are produced solely from anthracene predicts <1 μM of oxygenated products. The simulations also show that anthraquinone must be produced competitively with anthrone. The addition of the second oxygen to anthrone may occur when the anthrone is bound to Ru (during the B → C phase of the reaction), while there is still **RuO**$^{2+}$ present.

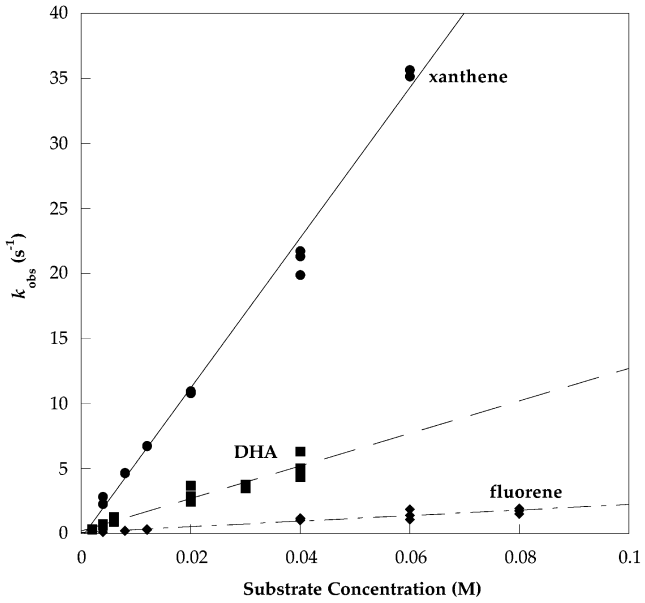

Figure 4. Plot of k_{obs} for A → B vs substrate concentration for reactions of **RuO**$^{2+}$ with xanthene (●), DHA (■), and fluorene (◆). Data are from three separate runs at each concentration.

Table 3. Properties of Organic Substrates and Their Rate Constants for Oxidation by **RuO**$^{2+}$

substrate	k (M^{-1} s^{-1})	BDE(C–H)[a] (kcal mol^{-1})	IE[b] (eV)	pK_a[d]
xanthene	5.77×10^2	75.5	7.65	41.0
DHA	1.25×10^2	78	n.a.	41.1
indene	1.08×10^1	78.9	8.14	20.1
fluorene	2.19×10^1	80	7.91	33.6
cyclohexene	9.2×10^{-1}	81.6[e]	8.95	
cumene[c]	3.3×10^{-2}	84.8[e]	8.73	
ethylbenzene[c]	2.2×10^{-2}	87[e]	8.77	
toluene	6.4×10^{-3}	90[f]	8.83	
anthracene	2.7×10^{-1}	~111[g]	7.44	

[a] From refs 27; errors ±~2 kcal mol^{-1}. [b] Reference 41 [c] Reference 19b. [d] Values measured in DMSO[42] and extrapolated to CH_3CN using the equation p$K_{a(C-H)}$ (CH_3CN) = 11 + p$K_{a(C-H)}$ (DMSO).[43] [e] Reference 44. [f] Reference 45. [g] DFT calculation.[46]

To check for the possible intermediacy of radicals in these reactions, the kinetics of xanthene oxidation by **RuO**$^{2+}$ were also examined in O_2-sparged MeCN solutions. Measurements were carried out in the stopped flow with 0.2 mM **RuO**$^{2+}$ and 20−60 mM xanthene. Data were analyzed as described above and gave the first-order rate $k_{xan,O2}$(A → B) = 340 ± 30 M^{-1} s^{-1}. This is a decrease in rate by almost half from the reaction rate under N_2 of $k_{xan} = 577 \pm 13$ M^{-1} s^{-1}. This is consistent with the involvement of carbon radicals that are trapped by O_2. The resulting peroxyl and perhaps oxyl radicals could then reoxidize **RuOH**$^{2+}$ or **RuOH$_2$**$^{2+}$, which would be observed as a slower rate of decay of oxidized ruthenium complexes.

The rates of oxidation of toluene, ethylbenzene, cyclohexene, and indene were similarly measured and analyzed with an A → B → C model. The values for the A → B phase are given in Table 3 (see below). The rate constant found for toluene oxidation, $k_{tol} = (6.4 \pm 0.6) \times 10^{-3}$ M^{-1} s^{-1}, is more than 2 orders of magnitude faster than the previously reported value of 5×10^{-5} M^{-1} s^{-1} (measured aerobically).[10] Potential origins of this discrepancy, and that some of the results reported in ref 10 have been difficult to reproduce in Meyer's labs and in our own, will be discussed elsewhere.[19] The oxidation of toluene

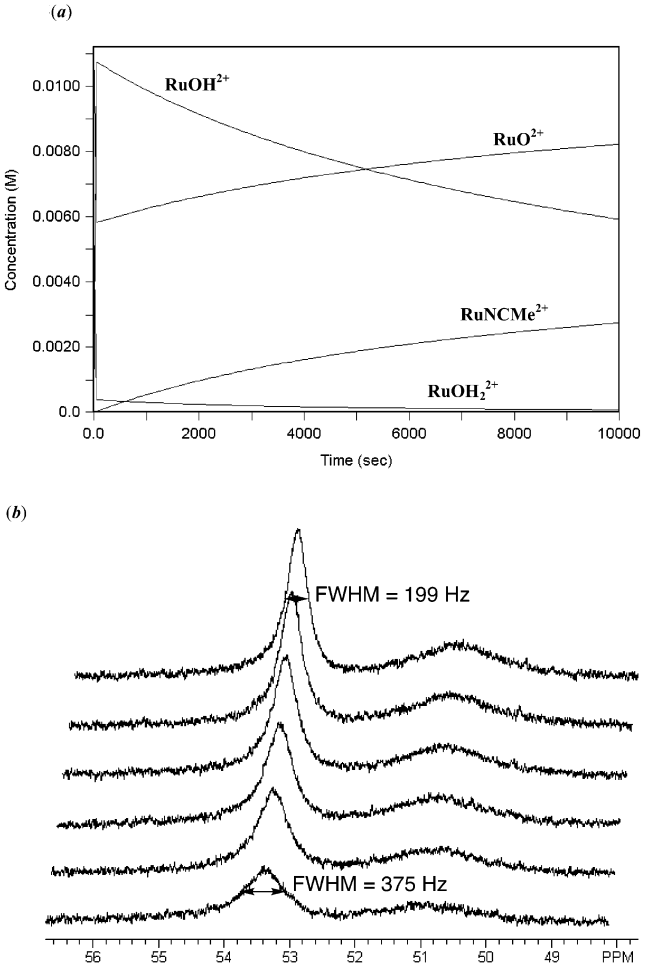

Figure 5. (a) Calculated concentrations over time for an NMR tube self-exchange reaction based on initial concentrations of 11.2 mM $\mathbf{RuO^{2+}}$ and 5.8 mM $\mathbf{RuOH_2^{2+}}$. (b) Stacked plot of ^{1}H NMR spectra from a $\mathbf{RuO^{2+}}$/$\mathbf{RuOH^{2+}}$ self-exchange experiment showing the sharpening of the $\mathbf{RuO^{2+}}$ resonance at δ53.5 from $t = 0$ to 2.5 h.

gives benzaldehyde—and possibly benzoic acid, though it was not observed by GC/FID or GC/MS. Indene and cyclohexene are oxidized on the stopped flow time scale (seconds) at $k_{ind} = 10.8 \pm 1$ M^{-1} s^{-1} and $k_{cyh} = 0.92 \pm 0.12$ M^{-1} s^{-1} to give indenone and cyclohexenone as the sole product in each case (by GC/MS). The rate constants are the same, within the error limits, as the values reported by Meyer and co-workers.[18] Oxidation of ethylbenzene gives exclusively acetophenone, with $k_{PhEt} = 2.2 \times 10^{-2}$ M^{-1} s^{-1}.

Deuterium isotope effects for the oxidation of DHA versus DHA-d_4 and toluene vs toluene-d_8 were measured over a range of concentrations and analyzed as above. Reaction of DHA-d_4 (98−99% deuterium enrichment as determined by ^{1}H NMR) gave $k_{DHA-d4} = 3.6 \pm 0.4$ M^{-1} s^{-1}, or $k_{DHA}/k_{DHA-d4} = 35 \pm 5$. Similarly, $k_{toluene-d8} = (9.56 \pm 0.18) \times 10^{-5}$ M^{-1} s^{-1} which gives $k_{toluene}/k_{toluene-d8} = 67 \pm 4$. Because these values are so large, the residual H contributes to the reactivity of the deuterated materials.[33] Taking this into account (but ignoring secondary isotope effects), the actual k_H/k_D for DHA is between 50 (calculated for 1% residual H) and 100 (for 2% residual H), and the 0.5% residual H in the methyl group of the toluene-d_8 gives an actual $k_H/k_D = 100$. A large deuterium isotope effect has been reported for $\mathbf{RuO^{2+}}$ oxidizing a CH vs CD bond in cyclohexene vs cyclohexene−d_4.[18]

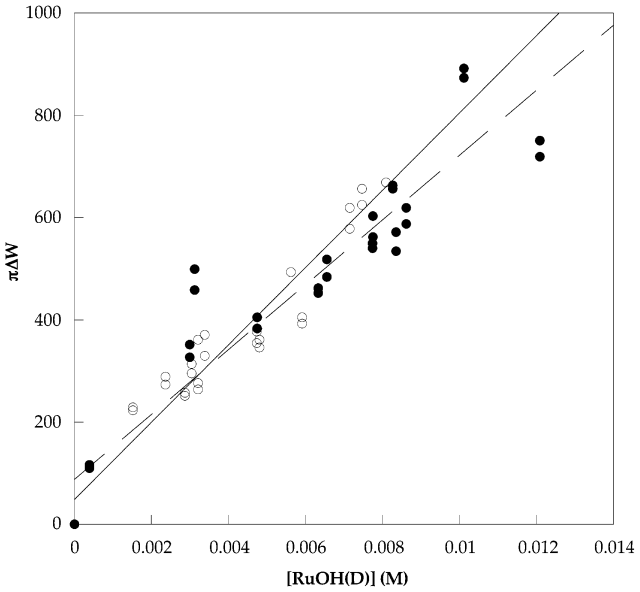

Figure 6. Plot of $\pi\Delta W$ vs [RuOH(D)] for the hydrogen-atom (○, −) and deuterium-atom (●, − −) self-exchange reactions (two runs each).

Self-Exchange Rates. Because the Marcus cross relation has been reported to hold for H-atom transfer reactions of this type, we have attempted to measure the rate of degenerate hydrogen-atom self-exchange between $\mathbf{RuO^{2+}}$ and $\mathbf{RuOH^{2+}}$ (eq 5) by dynamic NMR methods.[34] This is a challenging measurement because $\mathbf{RuOH^{2+}}$ is not stable in acetonitrile, undergoing disproportionation (eq 6)[6,35] and the resulting aquo complex solvolyzes to $\mathbf{RuNCMe^{2+}}$ as noted above. We have used this instability to prepare the solutions for the self-exchange study, as follows.

$$\mathbf{*RuO^{2+} + RuOH^{2+} \xrightarrow{k_{HSE}} *RuOH^{2+} + RuO^{2+}} \quad (5)$$

$$\mathbf{RuO^{2+} + RuOH_2^{2+} \underset{k_r = 80.6\ M^{-1}\ s^{-1}}{\overset{k_f = 4.07 \times 10^3\ M^{-1}\ s^{-1}}{\rightleftharpoons}} 2RuOH^{2+}} \quad (6)$$

In CD_3CN solution, addition of 0.5 equiv $\mathbf{RuOH_2^{2+}}$ to 1 equiv of $\mathbf{RuO^{2+}}$ forms a solution of roughly equimolar $\mathbf{RuO^{2+}}$ and $\mathbf{RuOH^{2+}}$, with a small amount of $\mathbf{RuOH_2^{2+}}$ ($K_{eq} = 50$ for eq 6). The presence of $\mathbf{RuOH^{2+}}$ results in the broadening of the proton resonances for the pyridyl ligands of $\mathbf{RuO^{2+}}$ because of the self-exchange reaction (eq 5). The small concentration of $\mathbf{RuOH_2^{2+}}$ slowly undergoes solvolysis in CD_3CN, causing the equilibrium to shift and the amount of $\mathbf{RuOH^{2+}}$ to decrease (Figure 5a). As a result, a range of concentrations of $\mathbf{RuOH^{2+}}$ occur over time in only one NMR tube. As the concentration of $\mathbf{RuOH^{2+}}$ decreases, the line widths of $\mathbf{RuO^{2+}}$ sharpen because the rate of self-exchange decreases (Figure 5b).

A plot of the increase in line width ($\pi\Delta W$) for two different resonances versus [$\mathbf{RuOH^{2+}}$] is roughly linear (Figure 6) suggesting that $\mathbf{RuO^{2+}}$ and $\mathbf{RuOH^{2+}}$ undergo chemical exchange on the NMR time-scale. This process is a net hydrogen-atom self-exchange as these complexes differ by a proton and

(33) For a discussion of the effect of residual H on observed k_H/k_D, see: Sorokin, A.; Robert, A.; Meunier, B. *J. Am. Chem. Soc.* **1993**, *115*, 7293−7299.
(34) Sandström, J. *Dynamic NMR Spectroscopy*; Academic Press: New York, 1982.
(35) For related studies of polypyridyl Ru^{IV}=O + $Ru^{II}(H_2O)$ reactions, see: (a) Iordanova, N.; Hammes-Schiffer, S. *J. Am. Chem. Soc.* **2002**, *124*, 4848−4856. (b) Farrer, B. T.; Thorp, H. H. *Inorg. Chem.* **1999**, *38*, 2497.

an electron. We have previously used this approach to measure H-atom self-exchange rates for iron complexes.[26,36] The data are consistent for two experiments with different batches of Ru starting materials, each measured at two different proton resonances. The slope of the line suggests an average self-exchange rate constant of $k_{HSE} = (7.6 \pm 0.4) \times 10^4\ M^{-1}\ s^{-1}$.

The same procedure was carried out with the addition of **Ru−OD$_2$**$^{2+}$ to determine the deuterium-atom self-exchange rate. The CD_3CN used in the experiment was dried thoroughly over CaH_2 and P_2O_5, and the NMR indicated only a small amount (<0.5 mM) of H_2O present in the solvent. As a check on the isotopic purity of the reaction mixture, the integral for H_2O in the CD_3CN reaction solution does not grow in appreciably through the experiment indicating nearly quantitative D_2O incorporation into the starting material [solvolysis of **RuO(H/D)$_2$**$^{2+}$ by CD_3CN increases the amount of free $(H/D)_2O$ in the sample]. A plot of the increase in line width ($\pi\Delta W$) for two different resonances versus [**Ru−OD**$^{2+}$] is linear and gives a self-exchange rate constant of $k_{DSE} = (6.4 \pm 0.4) \times 10^4\ M^{-1}\ s^{-1}$ (Figure 6). This gives a self-exchange isotope effect $k_{HSE}/k_{DSE} = 1.2 \pm 0.1$. This small isotope effect raises the question of whether the NMR line broadening really results from the self-exchange reaction or is due to some other process. Two different resonances of **RuO**$^{2+}$ broaden equally, consistent with an exchange process. But it is difficult to obtain direct evidence for exchange, such as peak coalescence, because of the instability of **RuOH**$^{2+}$. Thus, the assignment of k_{HSE} as $(7.6 \pm 0.4) \times 10^4\ M^{-1}\ s^{-1}$ should be considered tentative (certainly an upper limit).

Discussion

Mechanistic Considerations. $[(bpy)_2(py)Ru^{IV}O]^{2+}$ (**RuO**$^{2+}$) is an extensively studied material that is known to oxidize a wide range of substrates.[3−22] A variety of mechanisms have been proposed for its oxidations of C−H and O−H bonds. Hydrogen-atom abstraction and related proton-coupled electron transfer (PCET) pathways have been proposed for **RuO**$^{2+}$ oxidations of O−H bonds (*e.g.*, hydroquinone,[5] H_2O_2,[9] and the comproportionation/disproportionation of eq 6)[6,8] but these have not been the suggested mechanisms for C−H bond oxidations. In detailed studies of allylic oxidation of cyclohexene and indene by **RuO**$^{2+}$, Meyer and co-workers considered a mechanism of H-atom abstraction followed by rapid radical trapping but concluded in favor of direct oxygen insertion because reactions of 3,3,6,6-tetradeuteriocyclohexene (d_4-cyclohexene) gave very little allylic rearrangement.[16,18] Oxidation of cyclohexene by **Ru^{III}OH**$^{2+}$, however, was concluded to proceed by H-atom abstraction.[18] Che and co-workers have suggested an H-atom abstraction mechanism for C−H bond oxidations by ruthenium(VI) dioxo complexes.[22b,d]

The oxidations of DHA, xanthene, and fluorene presented here give both oxygenated (anthrone, anthraquinone, xanthone, fluorenone) and non-oxygenated products (anthracene, 9,9′-bixanthene, bifluorene). The oxygen in the products does not come from water (as shown by added $H_2{}^{18}O$ experiments), so under our anaerobic conditions, it must come from the ruthenium-oxo group. The formation of bixanthene and bifluorene by **RuO**$^{2+}$ indicates the intermediacy of radicals in these processes in sufficient concentrations to dimerize. Addition of O_2 to the reaction solutions causes a change in the rate of the first (A → B) phase of xanthene oxidation $k_{A\rightarrow B}$, indicating that organic radicals are involved in the A → B phase when **RuO**$^{2+}$ is being consumed. The large deuterium isotope effect for the oxidation of DHA-d_4 ($k_H/k_D \geq 35 \pm 1$) indicates that C−H bond breaking is an important part of the rate-limiting step. Isotope effects of this magnitude are often attributed to tunneling and have been observed in many other oxidations by **RuO**$^{2+}$,[9b,12,13] including $k_H/k_D = 21 \pm 1$ for the oxidation of cyclohexene vs cyclohexene-d_4.[18]

The data indicate that at least a portion of the reactions of **RuO**$^{2+}$ proceed by initial H-atom abstraction. A mechanism that involves solely oxygen atom insertion by **RuO**$^{2+}$, and formation of radicals only by **RuOH**$^{2+}$ is difficult to rationalize with the effect of oxygen on the rate and the higher yield of radical coupling products at higher xanthene and fluorene concentrations (see below). The high yield of the non-oxygenated product anthracene would have to be explained by dehydration of an intermediate 9,10-dihydroanthracenol complex to anthracene and **RuOH$_2$**$^{2+}$ [37] competitive with its oxidation to anthrone. The significant formation of Ru^{III} intermediates in the oxidation of DHA (observed in spectrum B) seems inconsistent with a two-electron oxygen-insertion pathway, since comproportionation of **RuO**$^{2+}$ with **RuOH$_2$**$^{2+}$ is slower than C−H bond oxidation under our conditions. For example, at 40 mM DHA and 0.2 mM **RuO**$^{2+}$, $t_{1/2}$ for the A → B phase of the oxidation is 0.13 s, whereas $t_{1/2} = 0.85$ s for reaction of **RuOH$_2$**$^{2+}$ with 0.2 mM **RuO**$^{2+}$. Xanthene is even faster.

It is possible that there is a mixed mechanism, with **RuO**$^{2+}$ reacting both by direct oxygen atom insertion and by hydrogen atom abstraction. However, there is no need to invoke direct oxygen insertion, as all of the data can be rationalized by an H-atom abstraction pathway as described in the following sections. It should be noted that there are few documented cases of direct O-atom insertion into C−H bonds,[38] whereas experiments have increasingly shown H-atom abstraction by metal-oxo and other complexes.[39] **RuO**$^{2+}$ and **RuOH**$^{2+}$ are thermodynamically good hydrogen atom abstractors, as they form O−H bonds of 84 and 82 ± 2 kcal mol^{-1} (Scheme 1). Direct oxygen transfer likely does occur in the oxidation of anthracene by **RuO**$^{2+}$. Aromatic oxidations in general do not proceed by hydrogen atom abstraction because the aromatic C−H bond is too strong (see Table 3). Most likely, **RuO**$^{2+}$ acts as an electrophile toward anthracene, analogous to the mechanism proposed for phenol oxidation by **RuO**$^{2+}$.[14] **RuO**$^{2+}$ is known

(36) Yoder, J. C.; Roth, J. P.; Gussenhoven, E. M.; Larsen, A. S.; Mayer, J. M. *J. Am. Chem. Soc.* **2003**; *125*, 2629−2640.

(37) (a) Rao, S. N.; More O'Ferrall, R. A.; Kelly, S. C.; Boyd, D. R.; Agarwallb, R. *J. Am. Chem. Soc.* **1993**, *115*, 5458−5465. (b) Dey, J.; O'Donoghue, A. C.; More O'Ferrall, R. A. *J. Am. Chem. Soc.* **2002**, *124*, 8561−8574.

(38) See, for example: (a) Chen, K.; Que, L., Jr. *J. Am. Chem. Soc.* **2001**, *123*, 6327−6337. (b) Shustov, G. V.; Rauk, A. *J. Org. Chem.* **1998**, *63*, 5413−5422 and Du, X.; Houk, K. N. *J. Org. Chem.* **1998**, *63*, 6480−6483, and references therein.

(39) See, for instance: (a) References 1c, 23−26, 29, 38a. (b) Cook, G. K.; Mayer, J. M. *J. Am. Chem. Soc.* **1994**, *116*, 1855−1868 (correction, *ibid.*, 8859). (c) Cook, G. K.; Mayer, J. M. *J. Am. Chem. Soc.* **1995**, *117*, 7139−7156. (d) Bryant, J. R.; Taves, J. E.; Mayer, J. M. *Inorg. Chem.* **2002**, *10*, 2769−2776. (e) Lockwood, M. A.; Blubaugh, T. J.; Collier, A. M.; Lovell, S.; Mayer, J. M. *Angew. Chem., Int. Ed. Engl.* **1999**, *38*, 225−227. (f) Mahapatra, S.; Halfen, J. A.; Tolman, W. B. *J. Am. Chem. Soc.* **1996**, *118*, 11 575−11 586. (g) Qin, K.; Incarvito, C. D.; Rheingold, A. L.; Theopold, K. H. *J. Am. Chem. Soc.* **2002**, *124*, 14 008−14 009. (h) Auclair, K.; Hu, Z.; Little, D. M.; Ortiz de Montellano, P. R.; Groves, J. T. *J. Am. Chem. Soc.* **2002**, *124*, 6020−6027 and references therein. (i) Reitz, J. B.; Solomon, E. I. *J. Am. Chem. Soc.* **1998**, *120*, 11 467−11 478. (j) Fontecave, M.; Pierre, J. L. *Comptes Rendus Acad. Sci. Ser. II C* **2001**, *4*, 531−538 "Mechanisms of Formation of Free Radicals In Biological Catalysis."

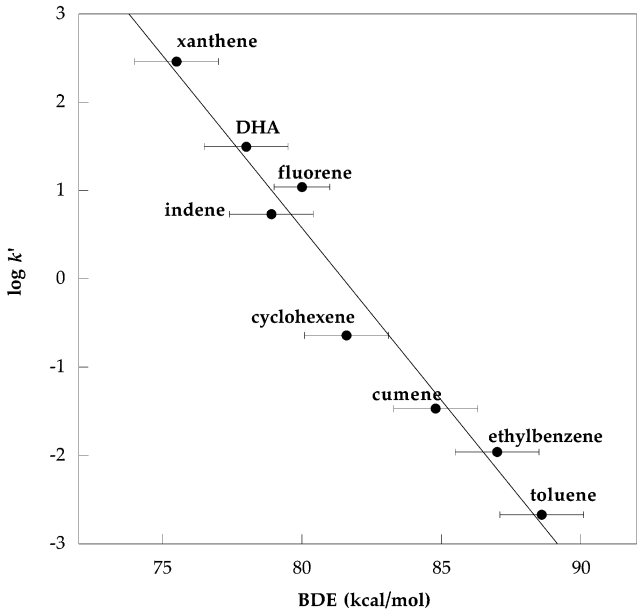

Figure 7. Plot of log k' vs BDE for oxidation of various substrates by $\mathbf{RuO^{2+}}$.

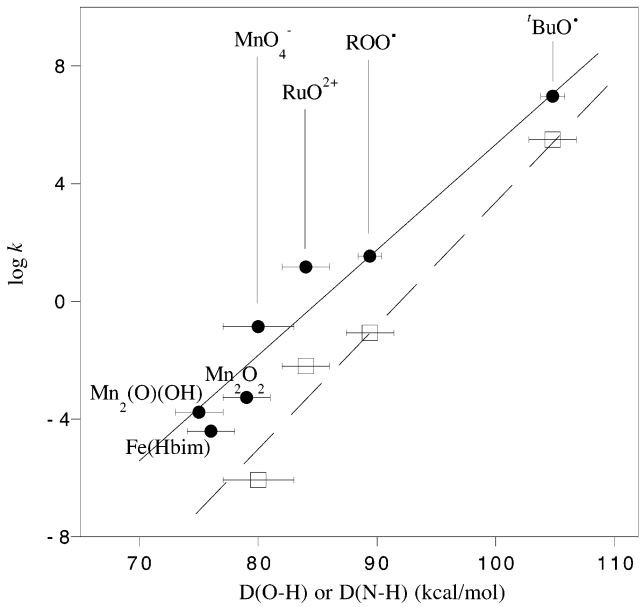

Figure 8. Plot of the log of the rate constant for H-atom abstraction for DHA (●, −) and toluene (○, − −) vs the strength of the X−H bond formed by the oxidant. The straight lines are drawn through the two oxygen radical points. Mn_2O_2 represents the value for oxidation by $[(phen)_2Mn^{IV}(O)_2Mn^{III}(phen)_2]^{3+}$, $Mn_2(O)(OH)$ for $[(phen)_2Mn^{III}(O)(OH)Mn^{III}(phen)_2]^{3+}$, and Fe-(Hbim) for $[Fe^{III}(Hbim)(H_2bim)_2]^{2+}$.[23,29]

to attack other electron-rich substrates such as phosphines, sulfides, and alkenes.[15,17]

Reactivity vs Thermodynamic Driving Force. A hallmark of hydrogen atom abstraction processes is that the rate constants correlate with C−H bond dissociation energies (BDEs).[40] A plot of rate constant vs BDE for all of the substrates studied here (except anthracene) is shown in Figure 7 (data in Table 3). The rate constants in this plot (k'_H) are $k_{A\rightarrow B}$ values that have been statistically corrected for the number of reactive hydrogens (e.g., DHA, 4; xanthene, 2; toluene, 3). The k'_H values have not, however, been corrected the stoichiometries of the reaction, that one H-atom transfer can lead to the reduction of more than one molecule of $\mathbf{RuO^{2+}}$.[29,39b,c] The A → B kinetic phase does include multiple steps, as noted above, but the magnitude of this correction is difficult to estimate. The close correlation of k'_H with BDE is quite good over a range of ca. 10^5 in rate constants. It encompasses both benzylic and allylic oxidations and includes primary, secondary, and tertiary C−H bonds. This correlation is strong evidence for a common hydrogen-atom abstraction mechanism for all of the substrates. The rates of oxidation, $k_{A\rightarrow B}$, do not correlate with other properties of the substrates, such as ionization energy (IE) or acidity (pK_a), as shown in Table 3. For instance, cyclohexene has a lower IE than toluene, but reacts more slowly. Similarly, indene and fluorene are much more acidic than xanthene or DHA, but react more slowly. The data indicate that the reactions do not occur by rate-limiting initial electron or proton transfer. This is not surprising, as $\mathbf{RuO^{2+}}$ is not basic[20a] and is a very poor electron-transfer oxidant.[4]

The rapid rate of DHA oxidation by $\mathbf{RuO^{2+}}$ is consistent with $\Delta H^\circ = -6 \pm 3$ kcal mol^{-1} for the hydrogen-atom transfer step. This value is based on the 78 kcal mol^{-1} C−H bond strength in DHA and the 84 kcal mol^{-1} bond strength in $\mathbf{RuOH^{2+}}$ (Table 3, Scheme 1). In previous studies of H-atom abstraction reactions, we have found that rate constants for metal complexes correlate well with the rate constants for the oxygen radicals ^{t}BuO• and ROO• (R = ^{t}Bu, ^{s}Bu).[23] The oxidations of DHA and toluene by $\mathbf{RuO^{2+}}$ fit reasonably well on these correlation lines (Figure 8). The $\mathbf{RuO-H^{2+}}$ bond strength of 84 kcal mol^{-1} is higher than the hydrogen-atom affinities of MnO_4^-,[29] $[Fe^{III}(Hbim)(H_2bim)_2]^{2+}$,[23b] and $[(phen)_2Mn(\mu\text{-}O)_2Mn(phen)_2]^{3+}$ (80, 76, and 79 kcal mol^{-1}, respectively).[23c] It should be noted that Stack and co-workers have reported an exception to this correlation.[25] The correlation is a special case of a more general Marcus treatment (see below).

Scheme 2

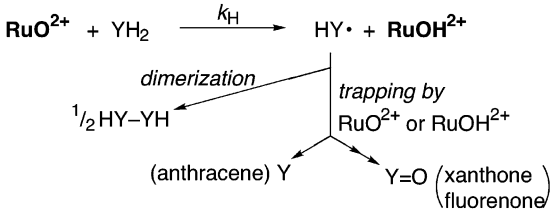

Product Formation. For xanthene and fluorene, the formation of both dimeric and oxygenated products indicates that radical coupling competes with trapping of the radical by the oxidant (Scheme 2). Oxidizing metal oxo compounds are known to be good radical traps, forming oxygenated products.[47] This trapping can compete with the almost diffusion controlled radical dimerization or disproportionation ($k_d \approx 10^9$ M^{-1} s^{-1})[48] because

(40) (a) *Free Radicals;* Kochi, J. K., Ed.; Wiley: New York, 1973, especially Ingold, K. U. Chapter 2, Vol 1, pp 67ff and Russell, G. A. Chapter 7, Vol. 1, pp 275−331. (b) Tedder, J. M. *Angew. Chem., Int. Ed. Engl.* **1982**, *21*, 401−410. (c) See also refs 23a and 25.

(41) http://webbook.nist.gov/chemistry: NIST Standard Reference Database Number 69−July 2001 Release.
(42) (a) Reference 27a. (b) Bordwell, F. G. *Acc. Chem. Res.* **1988**, *21*, 456−463 and references therein.
(43) Wayner, D. D. M.; Parker, V. D. *Acc. Chem. Res.* **1993**, *26*, 287−294.
(44) Denisov, E. T.; Denisova, T. G. *Handbook of Antioxidants*, 2nd ed.; CRC Press: Boca Raton, 2000; p 21−36.
(45) Bierbaum, V.; DePuy, C.; Davico, G.; Ellison, B. *Int. J. Mass Spectrom. Ion Phys.* **1996**, *156*, 109−131.
(46) Barckholtz, C.; Barckholtz, T. A.; Hadad, C. M. *J. Am. Chem. Soc.* **1999**, *121*, 491−500.

Scheme 3. Kinetic Models for Oxidations of Xanthene (XH_2) and Fluorene (FlH_2) by $\mathbf{RuO^{2+}}$

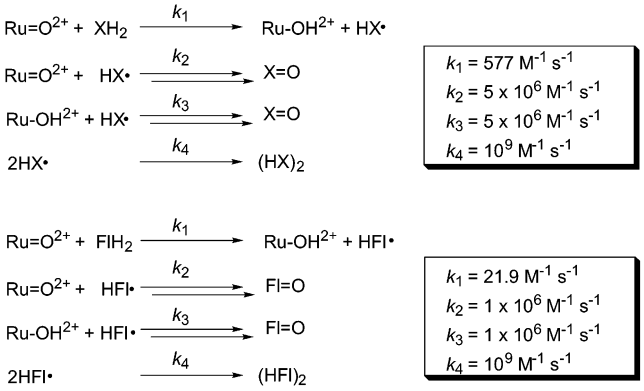

Table 4. Experimental and Calculated Product Concentrations Using the Model in Scheme 3[a]

		[(HY)$_2$] (mM)[a]		[Y=O] (mM)[a]	
	[$\mathbf{RuO^{2+}}$]:[YH_2](mM)	observed[b]	calculated	observed[b]	calculated
Xanthene:	1:1	0.013	0.010	0.36	0.38
	1:2	0.019	0.010	0.35	0.38
	1:4	0.025	0.021	0.31	0.38
	1:10	0.036	0.043	0.38	0.36
	2:4	0.045	0.017	0.66	0.76
	4:4	0.045	0.020	1.31	1.55
Fluorene:	1:1	0.011	0.006	0.37	0.49
	1:2	0.014	0.014	0.33	0.49
	1:4	0.017	0.026	0.31	0.47
	1:10	0.023	0.053	0.33	0.45
	2:4	0.027	0.027	0.63	0.97
	4:4	0.027	0.025	1.25	1.97

[a] (HY)$_2$ is 9,9′-bixanthene or bifluorene; Y=O is xanthone or fluorenone. [b] From Table 2.

the oxidant is present in much higher concentration than the radical. This model explains why the yield of dimerization products decreases with increasing concentrations of $\mathbf{RuO^{2+}}$ (Table 2). Addition of R$^\bullet$ to the oxo group in $\mathbf{RuO^{2+}}$ or to the hydroxo group in $\mathbf{RuOH^{2+}}$ would form $[(bpy)_2(py)Ru^{III}OR]^{2+}$ or $[(bpy)_2(py)Ru^{II}(HOR)]^{2+}$, consistent with the observed spectra. Further oxidation of these species and solvolyses, occurring typically in the slower kinetic phases such as B → C, generate the ketone and ruthenium products observed. The sensitivity of $k_{B\rightarrow C}$ to reaction conditions reflects the changing mixture of the processes occurring in this step.

The mechanism in Scheme 2 has been modeled for the xanthene and fluorene reactions using SPECFIT simulations (Scheme 3). In both cases, the k_1 steps are taken as the measured $k_{A\rightarrow B}$. The trapping rates, assumed for simplicity to be the same for $\mathbf{RuO^{2+}}$ and $\mathbf{RuOH^{2+}}$, need to be 5×10^6 M^{-1} s^{-1} for xanthenyl radicals and 1×10^6 M^{-1} s^{-1} for fluorenyl radicals to account for observed product ratios. A test of the model is that it reproduces the trends in ketone vs dimer yields on varying the initial concentrations (Table 4). A similar model was used in our study of oxidations by manganese μ-oxo dimers, which found trapping rates of 10^3-10^4 M^{-1} s^{-1}.[23c] In both that study and this work, trapping of xanthenyl radicals is faster than that of fluorenyl radicals, although the reason for this is not known.

In the oxidation of DHA, trapping of the hydroanthracenyl radical (HA$^\bullet$) can occur by either C−O bond formation or by transfer of a second hydrogen atom. The former path leads to anthrone and anthraquinone, and the latter gives anthracene. Anthracene can also be formed by disproportionation of two hydroanthracenyl radicals ($2HA^\bullet \rightarrow A + DHA$, $k_{disp} \approx 10^9$ M^{-1} s^{-1}).[48] Hydrogen transfer from HA$^\bullet$ is facile because of the very weak C−H bond strength in this radical, 43 kcal mol^{-1}.[49]

Meyer and co-workers ruled out a hydrogen atom transfer mechanism for the allylic oxidation of cyclohexene because reactions of 3,3,6,6-tetradeuteriocyclohexene (d_4-cyclohexene) gave very little allylic rearrangement.[18] For this result to be consistent with Scheme 2, the d_3-cyclohexenyl radical would have to be trapped rapidly by $\mathbf{RuOH^{2+}}$, within the solvent cage. Groves and co-workers had previously found 30% allylic rearrangement in the oxidation of this d_4-cyclohexene with cytochrome P450 enzymes and with an iron-porphyrin + iodosylbenzene catalytic system.[50] They argued on this basis for a rebound mechanism[51] analogous to Scheme 2.[50] The Groves result suggests that 60% of the cyclohexyl radicals have enough lifetime to be trapped randomly at either allylic position, but also that 40% of the oxidized products are formed regiospecifically, presumably by very rapid trapping. Similar explanations have been given for a number of C−H bond oxidations by Cr^{VI} and Mn^{VII} reagents that occur with partial retention of configuration, starting with a report by Wiberg in 1961.[52] These studies thus provide precedent for trapping that is sufficiently rapid that rearrangement is not observed. However, it is not clear why trapping of cyclohexenyl radicals by $\mathbf{RuOH^{2+}}$ would so efficient. With other hydrocarbon substrates, cage escape competes with trapping within the solvent cage, as indicated by the formation of dimeric products and the effect of O_2.

It should be noted that hydrogen atom abstraction and direct insertion are extremes of a mechanistic continuum. Many current theoretical treatments of C−H bond hydroxylation by metal-oxo species show that O−H bond formation and C−H bond cleavage occur prior to significant C−O bond formation, in part because the light hydrogen atom moves more quickly.[53] C−O bond formation often has a very small or essentially zero reaction barrier. Thus, it seems possible that rate constants for a set of processes could reflect an H-atom transfer rate-limiting step, whereas selectivities could suggest direct insertion.[54]

(47) (a) Steenken, S.; Neta, P. *J. Am. Chem. Soc.* **1982**, *104*, 1244−1248. (b) Al-Sheikhly, M.; McLaughlin, W. L. *Radiat. Phys. Chem.* **1991**, *38*, 203−211. (c) Libson, K.; Sullivan, J. C.; Mulac, W. A.; Gordon, S.; Deutsch, E. *Inorg. Chem.* **1989**, *28*, 375−377. (d) Elliot, A. J.; Padamshi, S.; Pika, J. *Can. J. Chem.* **1986**, *64*, 314−320. (e) References 23c, 29, 39b,c.

(48) Arends, I. W. C. E.; Mulder, P.; Clark, K. B.; Wayner, D. D. M. *J. Phys. Chem.* **1995**, *99*, 8182−8189.

(49) The sum of the H−AH bond strength (78 kcal mol^{-1}) and the H−A bond strength equals $\Delta H°$ for $H_2A \rightarrow A + 2$ H (A = anthracene). The $\Delta H°$ can be determined from $\Delta H°_f$ (H) = 52.1 kcal mol^{-1} and $\Delta H°$ for DHA → anthracene + H_2 = 17 kcal mol^{-1} (Cox, J. D.; Pilcher, G. *Thermochemistry of Organic and Organometallic Compounds*; Academic Press: New York, 1970).

(50) Groves, J. T.; Adhyam, D. V. *J. Am. Chem. Soc.* **1984**, *106*, 2177−2181.

(51) (a) Reference 39h and references therein. (b) Schoneboom, J. C.; Lin, H.; Reuter, N.; Thiel, W.; Cohen, S.; Ogliaro, F.; Shaik, S. *J. Am. Chem. Soc.***2002**, *124*, 8142−8151.

(52) Oxidation of (+)-3-methylheptane by chromic acid in 91% acetic acid gave the corresponding tertiary alcohol with 70−85% retention of configuration: Wiberg, K. B.; Foster, G. *J. Am. Chem. Soc.* **1961**, *83*, 424. (b) Oxidation of optically active PhCHDEt by CrO_2Cl_2 gives optically active 1-chloro-1-phenylpropane in 35−40% chemical yield and with about 35% retention of configuration: Stephenson, L. M.; Egnatchik, J.; Speth, D. R. *J. Org. Chem.* **1979**, *44*, 346−349. (c) Permanganate oxidations of arylvaleric acids gave 30−40% retention: Brauman, J. I.; Pandell, A. J. *J. Am. Chem. Soc.* **1970**, *92*, 329−335. See also: (d) Wiberg, K. B.; Fox, A. S. *J. Am. Chem. Soc.* **1963**, *85*, 3487. (e) Eastman, R. H.; Quinn, R. A. *J. Am. Chem. Soc.* **1960**, *82*, 4249.

(53) See, for instance: (a) Ogliaro, F.; Harris, N.; Cohen, S.; Filatov, M.; de Visser, S. P.; Shaik, S. *J. Am. Chem. Soc.* **2000**, *122*, 8977−8989. (b) Hata, M.; Hirano, Y.; Hoshino, T.; Tsuda, M. *J. Am. Chem. Soc.* **2001**, *123*, 6410−6416. (c) Baik, M.-H.; Gherman, B. F.; Friesner, R. A.; Lippard, S. J. *J. Am. Chem. Soc.* **2002**, *124*, 14 608−14 615. (d) Strassner, T.; Houk, K. N. *J. Am. Chem. Soc.* **2000**, *122*, 7821−7822.

Self-Exchange Rates and Application of the Marcus Cross Relation. We have recently shown that rate constants for a broad set of hydrogen atom transfer reactions XH + Y follow the Marcus cross relation (eq 7) fairly well.[26a,55] The correlations of rate constants with bond strengths in Figures 7 and 8 are special cases of the Marcus equation and cross relation, that hold

$$k_{XY} = \sqrt{k_{XX}k_{YY}K_{XY}f_{XY}} \quad (7)$$

when the intrinsic barriers are roughly constant across the series (or vary linearly with ΔG). The intrinsic barriers appear in eq 7 primarily through the rate constants for degenerate self-exchange XH + X (k_{XX}). The factor f_{XY} is close to unity for reactions of moderate driving-force.[55]

The applicability of the Marcus cross relation to the oxidation reactions described here can be tested using the rate of toluene oxidation by $\mathbf{RuO^{2+}}$. Benzyl radical + toluene self-exchange (k_{YY}) occurs with a rate constant of $\sim 1 \times 10^{-5}$ M^{-1} s^{-1} per hydrogen.[56] H-transfer from $PhCH_3$ to $\mathbf{RuO^{2+}}$ is 6 ± 3 kcal mol^{-1} uphill, based on D($PhCH_2$−H) = 90 kcal mol^{-1} and D(RuO−H) = 84 kcal mol^{-1}. Assuming $\Delta S = 0$ for the H-atom transfer, the $\Delta H°$ corresponds to an equilibrium constant of 4×10^{-5}, with an uncertainty of about 2 orders of magnitude. Using the tentative $\mathbf{RuO^{2+}}$/$\mathbf{RuOH^{2+}}$ self-exchange rate constant $k_{HSE} = 7.6 \times 10^4$ M^{-1} s^{-1} discussed above, and $f_{XY} = 1$,[57] gives $k_{calc}(\mathbf{RuO^{2+}} + PhCH_3) = 5.6 \times 10^{-3}$ M^{-1} s^{-1}. This is remarkably close to the experimental rate constant (per hydrogen) of 2.1×10^{-3} M^{-1} s^{-1}, a factor of 3 larger. As an alternative estimate of the $\mathbf{RuO^{2+}}$/$\mathbf{RuOH^{2+}}$ self-exchange rate, one could use the geometric mean of the comproportionation/disproportionation rate constants in eq 6, because these are close to self-exchange reactions ($\Delta G° = \pm 2.3$ kcal mol^{-1}).[6] Using this mean value ($k'_{HSE} = 5.7 \times 10^2$ M^{-1} s^{-1}), $k_{calc}(\mathbf{RuO^{2+}} + PhCH_3) = 4.9 \times 10^{-4}$ M^{-1} s^{-1}, a factor of 4 smaller than the experimental value. Thus, both estimates based on the cross relation are within the uncertainty of this calculation of a little more than an order of magnitude (primarily from uncertainties in the bond strengths used to estimate K_{eq}). It should be noted that while the Marcus cross relation is valuable for hydrogen atom transfer reactions in some ways, it does not provide an explanation of the large isotope effects. For instance, the k(toluene)/k(toluene-d_8) of $\sim 10^2$ would require that the isotope effect on toluene/benzyl radical self-exchange be an unrealistic 10^4.

Conclusions

$[(bpy)_2(py)Ru^{IV}O]^{2+}$ ($\mathbf{RuO^{2+}}$) oxidizes C−H bonds of alkyl-aromatic and allylic substrates, forming oxygenated products (such as xanthone), a dehydrogenated product (anthracene), and/or products from radical coupling (9,9′-bixanthenyl). The kinetic and mechanistic data are consistent with a mechanism of initial hydrogen-atom abstraction from the substrate to the ruthenium oxo group, to give $\mathbf{RuOH^{2+}}$ and the organic radical. This radical can be trapped by the oxidant or can encounter another radical to form dimerization products (Scheme 2). Rate constants for the initial hydrogen-atom transfer step correlate well with the strength of the C−H bond being cleaved, over a range of 10^5 in k. $\mathbf{RuO^{2+}}$ reacts slightly more slowly than ROO•, consistent with its 84 kcal mol^{-1} affinity for a hydrogen atom being smaller than that of the oxygen radical (90 kcal mol^{-1}; see Figure 8). ^{1}H NMR line-broadening experiments have given a tentative value of the $\mathbf{RuO^{2+}}$/$\mathbf{RuOH^{2+}}$ hydrogen-atom self-exchange rate constant k_{HSE}. Using this value, or an alternative estimate of k_{HSE}, the rate constant for H-atom transfer from toluene to $[(bpy)_2(py)Ru^{IV}O]^{2+}$ is well predicted by the Marcus cross relation.

Experimental Section

General Considerations. All experiments were performed under an N_2 atmosphere using standard techniques unless otherwise noted. Solvents (including deuterated solvents from Cambridge Isotope) were degassed and dried according to standard procedures.[58] Acetonitrile (low-water brand) was purchased from Burdick and Jackson and dispensed from a stainless steel keg plumbed directly into the drybox. CD_3CN was stirred over CaH_2 for 2 days, vacuum transferred to P_2O_5 and stirred for 4 h. It was then transferred back to CaH_2, stirred for 30 min, and transferred to a sealable flask prior to use. Dihydroanthracene (DHA) was recrystallized twice from absolute ethanol. Other reagents were purchased from Aldrich and used as received unless otherwise noted. $Ru(bpy)_2Cl_2$ and $[Ru(bpy)_2(py)Cl](PF_6)$ were synthesized according to literature methods.[20a,59] $[Ru(bpy)_2(py)(OH_2)](PF_6)_2$ ($\mathbf{RuOH_2^{2+}}$) and $[Ru(bpy)_2(py)O](PF_6)_2$ ($\mathbf{RuO^{2+}}$) were synthesized by modified literature procedures. The same procedure for the synthesis of the perchlorate salt $[Ru(bpy)_2(py)(OH_2)](ClO_4)_2$ was followed,[20b] except that a saturated solution of KPF_6 in water was used to precipitate the product. A procedure similar to the one used to synthesize $[Ru(bpy)_2(py)^{18}O](ClO_4)_2$ was used[13a] to produce $[Ru(bpy)_2(py)O](PF_6)_2$. Liquid Br_2 was added in a very small amount to the dissolved $\mathbf{RuOH_2^{2+}}$ and the resulting solution was purged with N_2 for several minutes. The solution was cooled and 1−2 mL of saturated KPF_6 in water was added to precipitate the product. $\mathbf{Ru{-}OD_2^{2+}}$ was synthesized in a manner identical to that used for the synthesis of $\mathbf{RuOH_2^{2+}}$ except that D_2O replaced H_2O at all points in the synthesis from $[Ru(bpy)_2(py)Cl](PF_6)$.[20b] Only one batch of $\mathbf{Ru{-}OD_2^{2+}}$ was synthesized and it was stored in a vial in the drybox between experiments. $\mathbf{RuO^{2+}}$, $\mathbf{RuOH^{2+}}$, $\mathbf{RuOH_2^{2+}}$, $\mathbf{Ru{-}OD_2^{2+}}$, and $\mathbf{RuNCMe^{2+}}$ were characterized by NMR and UV−vis spectroscopies.[20] DHA-d_4 was synthesized by a previous member of the lab by exchange of protons with sodium dimsylate-d_5 in DMSO-d_6.[60]

^{1}H NMR spectra were recorded on Bruker AC-200, AF-300, and DRX-500 spectrometers at ambient temperatures and are reported in ppm relative to $SiMe_4$. UV−vis spectra were recorded on a Hewlett-Packard 8453 diode array spectrophotometer and are reported as λ_{max} (nm), (ϵ, M^{-1} cm^{-1}). GC/MS data were obtained on a Hewlett-Packard 5971 instrument equipped with a nonpolar capillary column and a mass spectral analyzer. GC/FID spectra were obtained on a Hewlett-Packard 5890 instrument equipped with a similar column. Yields of organic products were quantified using response factors and confirmed by the addition of authentic samples.

Typical Procedure for Organic Oxidations. A solution of **xanthene** (4 mg, 20 μmol) and $\mathbf{RuO^{2+}}$ (5 μmol) in 5 mL MeCN turned orange

(54) (a) This argument is related to one made by Groves, personal communication, ref 39h, and Brazeau, B. J.; Austin, R. N.; Tarr, C.; Groves, J. T.; Lipscomb, J. D. *J. Am. Chem. Soc.* **2001**, *123*, 11 831−11 837. (b) Related arguments have been in the context of dioxirane oxidations, cf., Curci, R.; Dinoi, A.; Fusco, C.; Lillo, M. A. *Tetr. Lett.* **1996**, *37*, 249−252.
(55) Marcus, R. A.; Sutin, N. *Biochim. Biophys. Acta* **1985**, *811*, 265−322.
(56) Jackson, R. A.; O'Neill, D. W. *J. Chem. Soc., Chem. Commun.* **1969**, 1210−1211.
(57) $\ln f_{xy} = [1/4(\ln K_{xy})^2]/[\ln(k_{xx}k_{yy}/Z^2)]$.[55] Using the values given above, with $Z = 10^{11}$ (ref 55), $f_{xy} = 0.98$.
(58) Perrin, D. D.; Armarego, W. L. F. *Purification of Laboratory Chemicals*, 3rd ed.; Pergamon Press: New York, 1988.
(59) Sullivan, B. P.; Salmon, D. J.; Meyer, T. J. *Inorg. Chem.* **1978**, *17*, 3334−3341.
(60) Bailey, R. J.; Card, P. J.; Schechter, H. *J. Am. Chem. Soc.* **1983**, *105*, 6096−6103.

within 5 min. 9,9′-Bixanthene was observed by GC/MS *m*/*z* 181, M^+ (at twice the retention time of xanthene), 152, 69, 39.[39d] Xanthone was observed at *m*/*z* 196, 168, 139. Oxidation of **fluorene** showed bifluorene (*m*/*z* 330, 165), bifluorenylidene (*m*/*z* 328), and fluorenone (*m*/*z* 180, 152). Oxidations of **DHA** were monitored by GC/MS and by UV−vis spectroscopy, where anthracene production was evident from its characteristic spectrum in CH_3CN: 359 (8800), 378 (8200) after removal of the Ru^{II} product by passing the solution through a silica pipet column. Anthracene was quantitated by UV−vis and by GC/FID response factors. Anthraquinone production was also observed by GC/MS (*m*/*z* 208, 180, 152). ^{18}O-labeling studies were conducted under the same conditions as above, but with 10mM added $H_2{}^{18}O$. The amount of ^{18}O incorporation was measured by comparing the M^+:$M + 2^+$ peak intensity ratios for products formed in the presence of $H_2{}^{18}O$ to those formed in the absence of $H_2{}^{18}O$.

Kinetics Studies. Stopped-flow kinetic data were obtained using an OLIS stopped flow apparatus with a rapid scanning monochromator, typically obtaining spectra from 350 to 650 nm every 0.001 to 0.5 s over 1−1000 s. Kinetic data were analyzed using the global analysis software package SPECFIT.[32] Reactions of $\mathbf{RuO^{2+}}$ with xanthene, fluorene and DHA were carried out with 0.2 mM $\mathbf{RuO^{2+}}$ and 2−80 mM substrate in MeCN. Solutions were made up in an N_2-filled drybox immediately prior to use. Oxidations of xanthene in O_2-saturated solution were carried out in the stopped flow instrument using acetonitrile sparged with O_2 prior to mixing with the reagents. The kinetics of anthracene oxidation by $\mathbf{RuO^{2+}}$ were slow enough to be carried out with the HP 8453 diode array spectrophotometer, monitoring every 2 s for 600 s. Solutions were made up and transferred to a cuvette with a Teflon Kontes valve in a nitrogen-filled glovebox.

Self-Exchange Measurements. The self-exchange rates for $\mathbf{RuO^{2+}}$/$\mathbf{RuOH^{2+}}$ and $\mathbf{RuO^{2+}}$/$\mathbf{Ru-OD^{2+}}$ were measured by dynamic ^1H NMR line broadening. A solution of 4.5 mg $\mathbf{RuO^{2+}}$ (5.6 μmol), 2.3 mg $\mathbf{RuOH_2^{2+}}$ (2.9 μmol) and 1 μL $(Me_3Si)_2O$ (as an internal standard) in 0.5 mL CD_3CN was prepared in a sealable NMR tube. ^1H NMR spectra were acquired every 10 min for 3−4 h. Line widths for $\mathbf{RuO^{2+}}$ were measured at δ 53.1 and −31.0 ppm by fitting to Lorentzian functions using the commercially available NUTS software (Acorn NMR). Values for ΔW were obtained by subtracting the natural line widths for $\mathbf{RuO^{2+}}$ in the absence of $\mathbf{RuOH^{2+}}$ from the values obtained by Lorentzian fitting.

Acknowledgment. We are grateful to Dr. Martin Sadilek and Dr. Brian Bales for assistance with mass spectra and chromatography and to Dr. T. J. Meyer and Dr. M. H. V. Huynh for sharing results prior to publication. We acknowledge the National Institutes of Health and the UW PRIME Fellowship for financial support.

Supporting Information Available: Kinetics traces and SPECFIT calculated spectra for the oxidation of fluorene, plots of log k vs log[x] for xanthene, DHA, and fluorene, Eyring plot for the oxidation of xanthene, and an overlay plot and kinetic trace for the oxidation of anthracene are included in the Supporting Information. This material is available free of charge via the Internet at http://pubs.acs.org.

JA035276W